Audio Engineering Society

Convention Paper 10223

Presented at the AES 158th Convention
2025 May 22–24, Warsaw, Poland

This paper was peer-reviewed as a complete manuscript for presentation at this convention. This paper is available in the AES E-Library (http://www.aes.org/e-lib), all rights reserved. Reproduction of this paper, or any portion thereof, is not permitted without direct permission from the Journal of the Audio Engineering Society.

Plane wave creation in non-spherical loudspeaker arrays using radius formulation by the Lamé function

Tomohiro Sakaguchi[1] and Yasuhiro Oikawa[1]

[1] *Waseda University*

Correspondence should be addressed to Tomohiro Sakaguchi (tommy0509@toki.waseda.jp)

ABSTRACT

This paper proposes the method for generating a plane wave field using spherical harmonics with a non-spherical array. In sound field control, arbitrary sound fields can be expanded into plane waves; thus, the sound field construction requires the plane wave generation. In conventional studies using spherical harmonics, plane wave reproduction has mainly been examined with circular or spherical arrays. However, considering the practical constraints of room geometry, plane wave generation in rectangular-like arrays is also important because loudspeakers are located along walls to use the space exhaustively. In this paper, we propose formulating the distance between the center and each loudspeaker using the Lamé function in a polar expression, by changing its order as well as the shape of spatial figures. This formulation allows us to reuse the same method applied to spherical arrays for configuring non-spherical arrays. As a result of the simulation experiment, it was confirmed that within the inscribed region, the proposed method using a higher-order Lamé function achieved waveform reproduction accuracy comparable to that of a spherical array.

1 Introduction

Sound field control methods are categorized into psycho-acoustic and physical modeling approaches [1]. In psycho-acoustic models, there are two main approaches: one where the positions of loudspeakers are constrained by ITU standards, such as the 5.1ch or 22.4ch formats [2] [3], and the other being the object-based, which allows some flexibility in loudspeaker placement. In such approaches, sound is primarily rendered as a phantom source, representing a sound originating from a non-existent loudspeaker. In Vector Base Amplitude Panning (VBAP) [4], the amplitude is replaced by a vector to control the position of the phantom source, with spatial information stored as metadata. Consequently, it is considered that discrepancies occur between the actual sound reproduction and the auditory perception. On the other hand, physical modeling approaches are based on the Kirchhoff-Helmholtz integral or the Rayleigh integral under an equal interval of each loudspeaker, such as Wave Field Synthesis (WFS) [5]. In addition, Ambisonics [6] is the sound field reproduction approach that uses spherical harmonics expansion. This multi-directional point microphone in orthogonal arrays, but the post-production area is limited to a single point. Thus, Sound field control in the physics literature is possible by the free arrangement of loudspeakers in the entire controllable space. A pressure field can be described in terms of plane waves [7]. The creation of plane wave has been proposed with spherical harmonics using an array of loudspeakers [8]. However, the analysis of spherical harmonics restricts the shape

of the loudspeaker array to a circle or a sphere, which reduces its flexibility of the array [9]. Considering the practical constraints of room geometry, plane wave generation in rectangular-like arrays is also important because loudspeakers are located along walls to use the space exhaustively. In this paper, we propose generation of plane wave fields with spherical harmonics for a cube-like array. We focus on the Lamé function, which defines an algebraic surface that transforms from a sphere to a cube by changing the order. It allows a non-spherical array to formulate the distance from the center. Simulation experiments are performed to evaluate the proposed method, which reduces the degradation of the waveform accuracy when compared to a higher order of the Lamé function.

2 Reproduction plane wave

We assume that $\mathbf{y}$ is the incident direction of a plane wave and $\mathbf{x}$ is the observation point. Unit vector expressed with hat on the spherical coordinate system, i.e. $\hat{\mathbf{x}} = [\cos\theta\sin\phi, \sin\theta\sin\phi, \cos\phi]^T$; therefore, the magnitude is given as $x = |\mathbf{x}| = \mathbf{x}/\hat{\mathbf{x}}$. A plane wave can be formulated as

$$S(\mathbf{x};k) = e^{ikx(\hat{\mathbf{y}}^T\hat{\mathbf{x}})}, \tag{1}$$

where $k = 2\pi f c^{-1}$ is the wave number, i is the imaginary unit. Thus, $S(\mathbf{x};k)$ represents the complex pressure of the ideal plane wave at $\mathbf{x}$ with the wave number k. Equation (1) can transfer with spherical harmonics as [7]

$$S(\mathbf{x};k) \approx \sum_{n=0}^{N}\sum_{m=-n}^{n} 4\pi X_n(kx)Y_{nm}^*(\hat{\mathbf{y}})Y_{nm}(\hat{\mathbf{x}}), \tag{2}$$

where N is the truncation number, $X_n(\cdot) \triangleq i^n j_n(\cdot)$, $j_n(\cdot)$ is the spherical Bessel function n th order, $Y_{nm}(\cdot)$ denotes the spherical harmonics as follows:

$$Y_{nm}(\cdot) = \sqrt{\frac{(2n+1)}{4\pi}\frac{(n-|m|)!}{(n+|m|)!}}P_{n|m|}(\cos\phi)e^{im\theta}, \tag{3}$$

where $P_{n|m|}(\cdot)$ is associated Legendre function, and $*$ denotes the complex conjugate. On the other hand, the generation of a plane wave with multi-loudspeakers is defined as [6]

$$T(\mathbf{x};k) = \sum_{l=1}^{L} a_l(k)|\mathbf{y}_l|e^{ik|\mathbf{y}_l|}\frac{e^{-ik|\mathbf{y}_l-\mathbf{x}|}}{|\mathbf{y}_l-\mathbf{x}|}, \tag{4}$$

where $\mathbf{y}_l$ represents the l th location of loudspeakers, and $a_l(k)$ is the l th loudspeaker amplitude coefficient in the wave number domain. With spherical harmonics, Eq. (4) can be rewritten in the form as [8]

$$T(\mathbf{x};k) \approx \sum_{n=0}^{N}\sum_{m=-n}^{n} 4\pi X_n(kx)R_n(kr) \times \sum_{l=1}^{L} a_l(k)Y_{nm}^*(\hat{\mathbf{y}}_l)Y_{nm}(\hat{\mathbf{x}}), \tag{5}$$

where $R_n(kr) \triangleq -ikre^{ikr}i^{-n}h_n(kr)$, and $h_n(\cdot)$ is the the n th order spherical Hankel function of the second kind. The difference from Eq. (2) is that $Y^{nm}(\cdot)$, which represents the direction of arrival of the plane wave, is replaced by the loudspeaker positions. This results in the term $R_n(kr)\sum_{l=1}^{L} a_l(k)Y_{nm}^*(\hat{\mathbf{y}}_l)$, which represents a single plane wave synthesized from multiple loudspeakers. Accordingly, the coefficients $a_l(k)$ must be computed based on the specific configuration of the loudspeaker array. The least squares problem is defined as [8]

$$\min_{\mathbf{a}}||\mathbf{P}\mathbf{a}-\mathbf{b}||^2, \tag{6}$$

where

$$\mathbf{P} = \begin{bmatrix} R_0(kr)\left[\mathbf{p}_{00}\odot\mathbf{e}_0\right] \\ R_1(kr)\begin{bmatrix}\mathbf{p}_{11}\odot\mathbf{e}_{-1}\\ \mathbf{p}_{10}\odot\mathbf{e}_0\\ \mathbf{p}_{11}\odot\mathbf{e}_1\end{bmatrix} \\ \vdots \\ R_N(kr)\begin{bmatrix}\mathbf{p}_{NN}\odot\mathbf{e}_{-N}\\ \vdots \\ \mathbf{p}_{NN}\odot\mathbf{e}_N\end{bmatrix}\end{bmatrix}, \tag{7}$$

$$\mathbf{a} = [a_1(k),\cdots,a_L(k)], \tag{8}$$

and

$$\mathbf{b} = \begin{bmatrix} P_{00}(\cos\phi)e^{-i0} \\ P_{11}(\cos\phi)e^{i\theta} \\ P_{10}(\cos\phi)e^{-i0} \\ P_{11}(\cos\phi)e^{-i\theta} \\ \vdots \\ P_{NN}(\cos\phi)e^{iN\theta} \\ \vdots \\ P_{NN}(\cos\phi)e^{-iN\theta}\end{bmatrix}, \tag{9}$$

where $\odot$ denotes Hadamard product. Equation (7) is the $(N+1)^2 \times L$ matrix which contains all spherical

harmonics information, and Eq. (8) is the L th vector of $a_l(k)$. Moreover, Eq. (9) is the $(N+1)^2$ th vector which has the target plane wave direction.

Furthermore, these vector, $\mathbf{p}_{nm}$ and $\mathbf{e}_m$, are defined as following:

$$\mathbf{p}_{nm} = [P_{n|m|}(\cos\phi_1), \cdots, P_{n|m|}(\cos\phi_L)], \tag{10}$$

$$\mathbf{e}_m = [e^{-im\theta_1}, \cdots, e^{-im\theta_L}]. \tag{11}$$

Equation (10) is the L th vector of Legendre function of each loudspeaker, and Eq. (11) is the Lth vector of the wave from each loudspeaker.

3 Proposed methods

3.1 Lamé function

The Lamé function is defined as an algebraic curve at cartesian coordinates. In three-dimensional, it can be described as

$$|x|^\alpha + |y|^\alpha + |z|^\alpha = |s|^\alpha, \tag{12}$$

where s is related to the magnitudes in the x, y and z directions, the order α affects its shape, and s contributes to the shape scale [10].

Figure 1 shows relationships between Lamé function and shape sliced at $z = 0$ with $s = 1.5$. In $\alpha = 2$, the shape is a circle. When α increases, the shape would be close to a cube. Equation (12) is converted to polar coordinates in a state with geometric meaning. This enables formulation the distances from the original point to the arbitrary point on each shape. The expression is given by

$$r(\alpha,\theta,\phi) = s(|\cos\theta\sin\phi|^\alpha + |\sin\theta\sin\phi|^\alpha + |\cos\phi|^\alpha)^{-\frac{1}{\alpha}}, \tag{13}$$

where θ is azimuth, and ϕ is elevation. In this paper, the polar axis is x axis, and the elevation is between z axis and $r(\alpha,\theta,\phi)$.

3.2 Lamé function for plane wave creation

According to $R_n(\cdot)$ in Eq. (5), it is interpreted as a radius function. Consequently, it is considered that the distances from the center to each loudspeaker can be incorporated into the function. As Fig. 1 and Eq. (13), the length of $r(\alpha,\theta,\phi)$ is not constant. Obviously, it

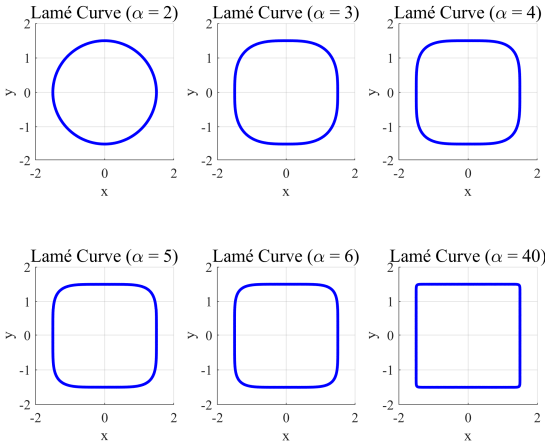


Fig. 1: Variables relation examples between lame function and shape in two-dimentional($s = 1.5$).

of circles or sphere, $\alpha = 2$, is known constant as radius. To use $r(\alpha,\theta,\phi)$ regardless of the array geometry, Eq. (5) can be revised as

$$T_{\mathrm{L}}(\mathbf{x};k) = \sum_{n=0}^{N}\sum_{m=-n}^{n} 4\pi X_n(kx) \times \sum_{l=1}^{L} a_l(k) Y^*_{nm}(\hat{\mathbf{y}}_l) R_n(kr(\alpha,\theta_l,\phi_l)) Y_{nm}(\hat{\mathbf{x}}). \tag{14}$$

The variable of R_n is replaced with $r(\alpha,\theta_l,\phi_l)$ so that it is merged into the summation over l. The term $\sum_{l=1}^{L} a_l(k) Y^*_{nm}(\hat{\mathbf{y}}_l) R_n(kr(\alpha,\theta_l,\phi_l))$ represents a single plane wave direction assuming a loudspeaker array configured based on the Lamé function. Therefore, so as to modify the calculation of $\mathbf{a}$, we introduce a vector as:

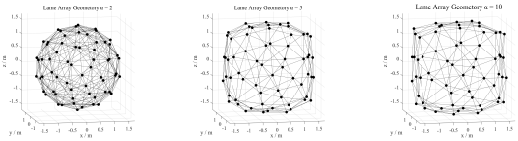
$$\mathbf{R}_n = [R_n(kr(\theta_1,\phi_1)), \cdots, R_n(kr(\theta_L,\phi_L))]. \tag{15}$$

Furthermore, the matrix (7) also is changed as:

$$\mathbf{P} = \begin{bmatrix} \mathbf{R}_0 \odot [\mathbf{p}_{00} \odot \mathbf{e}_0] \\ \mathbf{R}_1 \odot \begin{bmatrix} \mathbf{p}_{11} \odot \mathbf{e}_{-1} \\ \mathbf{p}_{10} \odot \mathbf{e}_0 \\ \mathbf{p}_{11} \odot \mathbf{e}_1 \end{bmatrix} \\ \vdots \\ \mathbf{R}_N \odot \begin{bmatrix} \mathbf{p}_{NN} \odot \mathbf{e}_{-N} \\ \vdots \\ \mathbf{p}_{NN} \odot \mathbf{e}_N \end{bmatrix} \end{bmatrix}. \tag{16}$$

Table 1: General conditions for all *Scenario*s.

	Value
Sound speed [m/s]	340
Sampling rate [Hz]	44100
Point resolution	300×300
Calculated space [m]	$-2 \leqq x \leqq 2, -2 \leqq y \leqq 2$
Value of s	1.5
Evaluation level	$z = 0$
Range Lamé order	$2 \leqq \alpha \leqq 10$



(a) $\alpha = 2$ **(b)** $\alpha = 5$ **(c)** $\alpha = 10$

Fig. 2: The array of loudspeaker in *Scenario* 1 and 2.

As a result, we can get the Lamé array coefficients by using Eq.(6). Finally, it assign to Eq. (14), we generate plane wave under Lamé array.

4 Simulation experiment

For all *Scenario*s, these 6 parameters are identical: the sound speed, the point resolution, the calculated space, the value of s, the evaluation level, and the range of the Lamé order. These are summarized in Table 1.

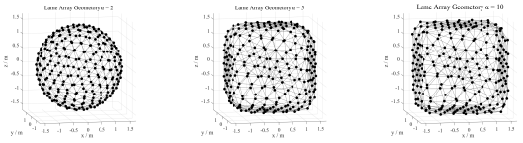
The each array was rearranged by extracting the angular information of the original sphere array and substituting them into Eq. (13). The sphere arrays are available from "SFS-Toolbox" [11] and were obtained by transforming the coordinate information.

4.1 Simulation conditions

Three scenarios were conducted via MATLAB simulations to verify the proposed method. Table 2 shows the simulation conditions.

Here, Fig. 2 and Fig. 3 show the geometry of the loudspeaker array on $L = 64, 256$ which is used at *Scenario* $1, 2$ and *Scenario* 3 through 6, respectively. The black dots indicate the speakers.

Scenario $1, 2$ are the sphere or cube-like geometry to compare under [8] condition. *Scenario* 3 through 6 increased the number of loudspeakers to 256 because



(a) $\alpha = 2$ **(b)** $\alpha = 5$ **(c)** $\alpha = 10$

Fig. 3: The array of loudspeaker in *Scenario* 3, 4, 5 and 6.

we had suggested a loudspeaker array system with the ability to operate the same number of loudspeakers as [12]. As mentioned in [8], the reason for the frequency selection is that for $L = 64$, the maximum reproduction frequency is 252 Hz, while for $L = 256$, it is 541 Hz.

4.2 Simulation results

Figure 4 - 9 show the waveforms at *Scenario* 1 through *Scenario* 6 extracting ideal and the Lamé order $\alpha = 2, 5, 10$. The black dots represent the boundary of the target region; the inside dots belong to the region. These figures indicate the acoustic pressures on real part calculated by Eq. (14), where its maximum value 1 is in yellow and minimum value -1 is in blue.

In *Scenario* 1 waveform, as shown in Fig. 4, Fig. 4b is the same condition as [8]. This proved the creation of a plane wave with Eq. (14). In addition, Fig. 4c and Fig. 4d confirmed that the plane wave creation is enabled when the Lamé order α increased.

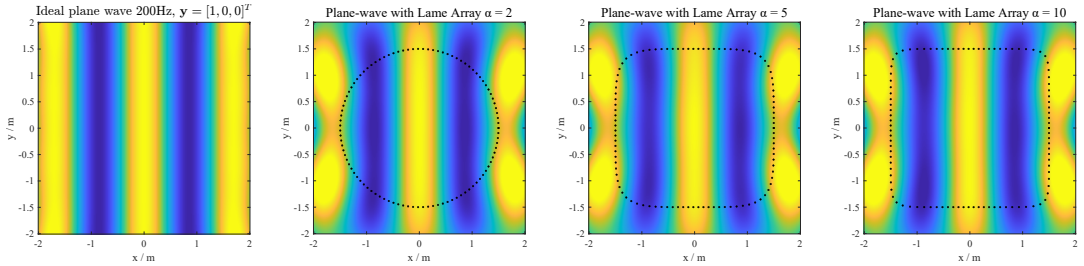
The *Scenario* 2 also results in successful plane wave creation. To verify effects at the corners of the loudspeaker array, the plane wave direction was selected. It was found that there is less impact on the waveform. The observation point is nearer to the region boundary, the waveform is more curve. This considered that all sound sources assumed point sources in Eq. (4). Furthermore, the expanded reproduction field keeps the waveform curve inside the region.

Scenario 3 compared with *Scenario* 1 in only changing the number of loudspeakers,and the same waveform resulted as *Scenario* 1. Similarly, *Scenario* 4 is also to verify the corner effect as well as *Scenario* 2, so that altering the number of loudspeakers is unrelated.

Figure 8 and 9 show that the plane wave creation is successful when the frequency is changed.

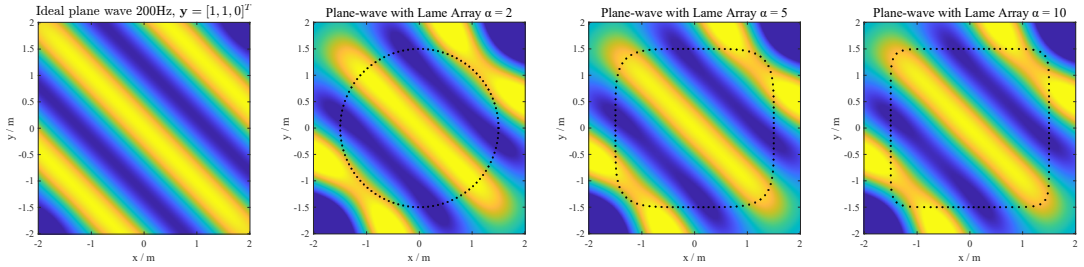
Table 2: Each simulation conditions for all *Scenario*s.

	Scenario 1	*Scenario* 2	*Scenario* 3	*Scenario* 4	*Scenario* 5	*Scenario* 6
Frequency [Hz]	200	200	200	200	500	500
Plane wave direction	[1, 0, 0]	[1, 1, 0]	[1, 0, 0]	[1, 1, 0]	[1, 0, 0]	[1, 1, 0]
Num. of loudspeaker	64	64	256	256	256	256
Spherical harmonics order	7	7	14	14	14	14



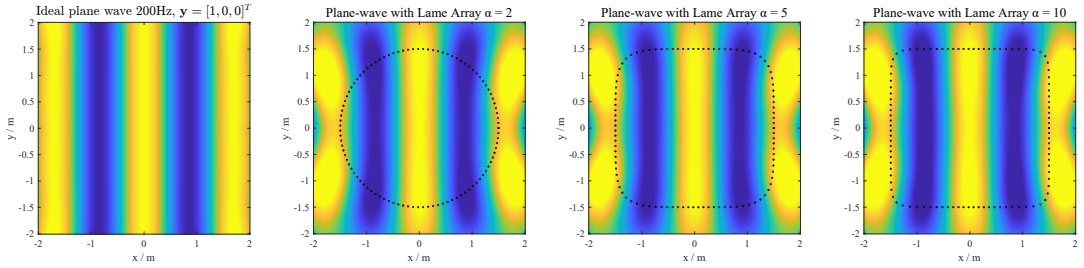
(a) Ideal **(b)** $\alpha = 2$ **(c)** $\alpha = 5$ **(d)** $\alpha = 10$

Fig. 4: Results of waveform in *Scenario* 1 at a height of $z = 0$



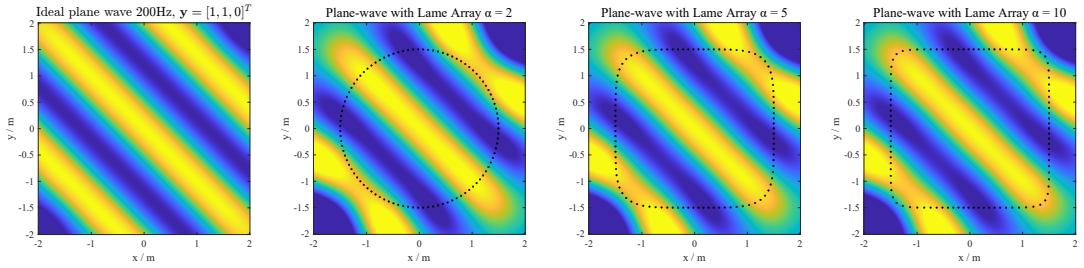
(a) Ideal **(b)** $\alpha = 2$ **(c)** $\alpha = 5$ **(d)** $\alpha = 10$

Fig. 5: Results of waveform in *Scenario* 2 at a height of $z = 0$.



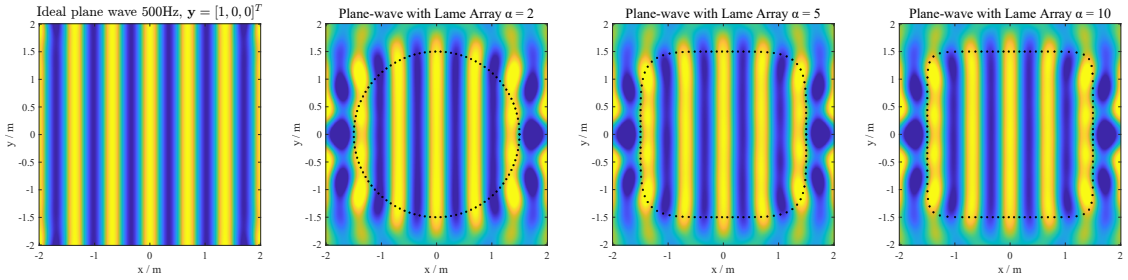
(a) Ideal **(b)** $\alpha = 2$ **(c)** $\alpha = 5$ **(d)** $\alpha = 10$

Fig. 6: Results of waveform in *Scenario* 3 at a height of $z = 0$.



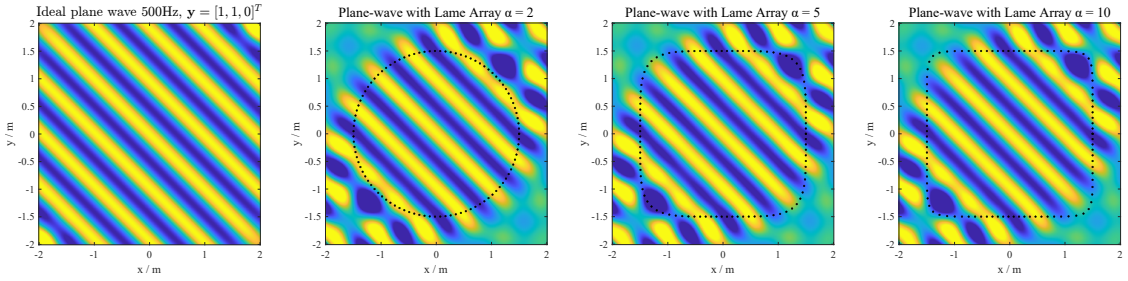
(a) Ideal **(b)** $\alpha = 2$ **(c)** $\alpha = 5$ **(d)** $\alpha = 10$

Fig. 7: Results of waveform in *Scenario* 4 at a height of $z = 0$.



(a) Ideal **(b)** $\alpha = 2$ **(c)** $\alpha = 5$ **(d)** $\alpha = 10$

Fig. 8: Results of waveform in *Scenario* 5 at a height of $z = 0$.



(a) Ideal **(b)** $\alpha = 2$ **(c)** $\alpha = 5$ **(d)** $\alpha = 10$

Fig. 9: Results of waveform in *Scenario* 6 at a height of $z = 0$.

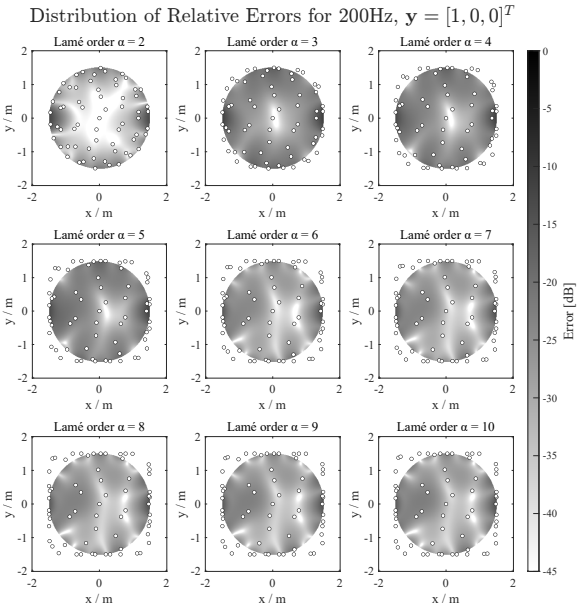


Fig. 10: Distribution error map of at *Scenario* 1.

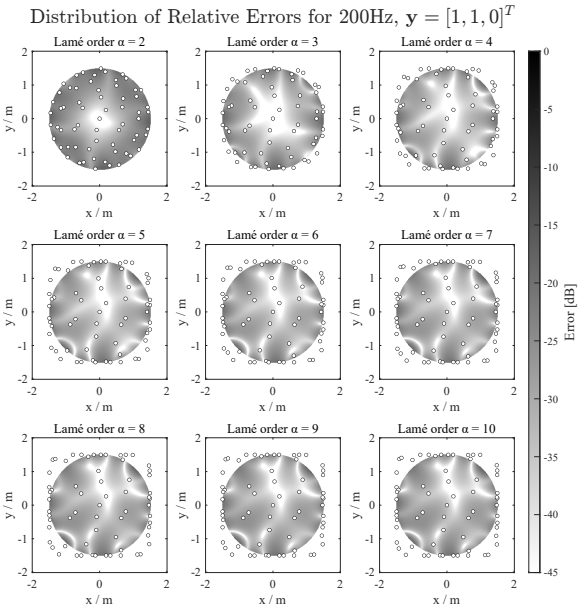


Fig. 11: Distribution error map of at *Scenario* 2.

5 Discussion

According to 4.2, the creation area does not expand by the reproduction region expansion. In this section, we mention inscribing each array considering rapidly the accuracy degradation. The error distribution is used to compare the accuracy of the generated wavefront with respect to the ideal wavefront for each evaluation point. This has an advantage in verifying visually the difference between the ideal plane wave and the created one. The value is calculated by

$$E_{\mathrm{dist}}(\mathbf{x};k) = 10\log_{10}\left(\frac{|S(\mathbf{x};k) - T_{\mathrm{L}}(\mathbf{x};k)|^2}{|S(\mathbf{x};k)|^2}\right). \quad (17)$$

Because it is desirable that $S(\mathbf{x};k)$ is close to $T_{\mathrm{L}}(\mathbf{x};k)$, the accuracy is higher if $E_{\mathrm{dist}}(\mathbf{x};k)$ is the lower. These distribution error maps are shown in Fig. 10 - 15 in *Scenario* 1 - *Scenario* 6, respectively.

Figure 10 represents the result of *Scenario* 1. For $\alpha = 2$, in whole area, the accuracy is the best under this condition. In contrast, it tends to be rapidly degraded off-center for $\alpha = 3, 4,$ and 5. Although there is some improvement with increasing the Lamé function order, the results of $\alpha = 6 - 10$ are inferior to those of $\alpha = 2$.

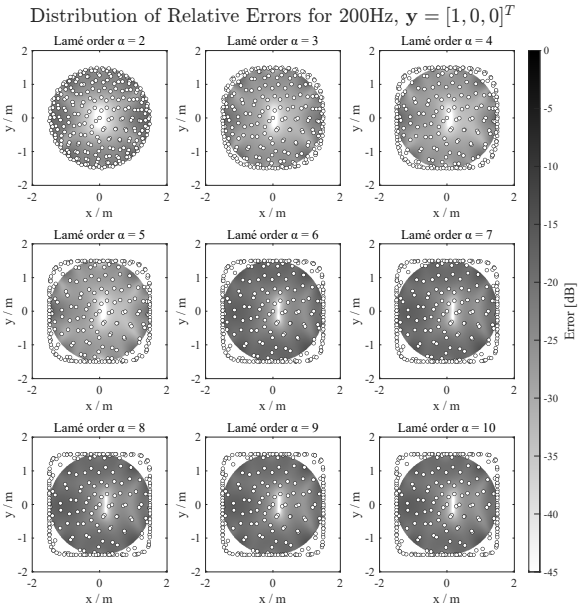


Fig. 12: Distribution error map of at *Scenario* 3.

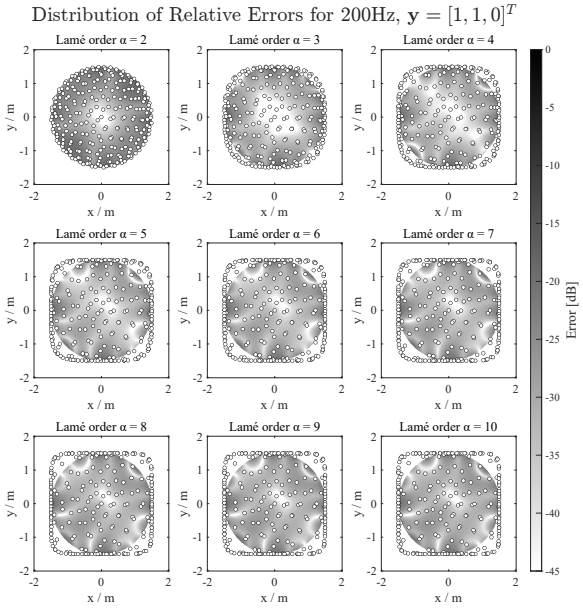


Fig. 13: Distribution error map of at *Scenario* 4.

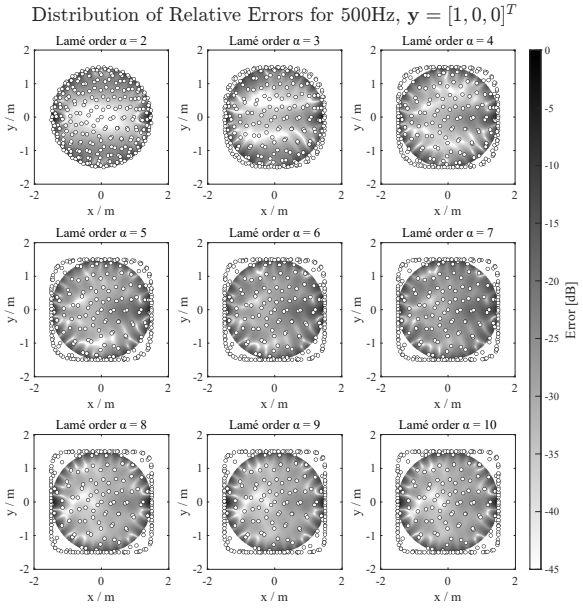


Fig. 14: Distribution error map of at *Scenario* 5.

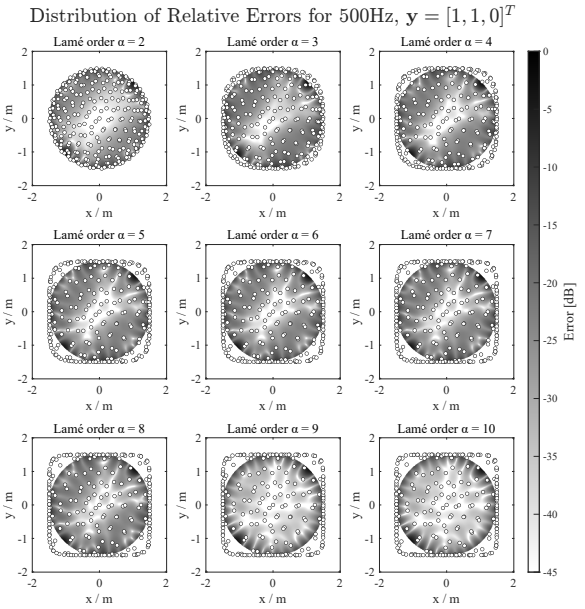


Fig. 15: Distribution error map of at *Scenario* 6.

The distribution of *Scenario* 2 is shown in Fig. 11. The $\alpha = 2$, spherical array, is the worst accuracy in *Scenario*s. Meanwhile, the Lamé function order is higher than $\alpha = 2$, and the quality of the waveform is ameliorated.

Figure 12 indicates the result of *Scenario* 3. The fidelity does not change in $\alpha = 2 - 5$, however, at least $\alpha = 6$, it extremely decreases.

Figure 13 behavior clearly corresponds to *Scenario* 2, hence *Scenario* 4 implied that the waveform does not depend on the number of loudspeakers in this condition.

The distribution maps are altered in Fig. 14 and 15 by changing frequency. In *Scenario* 5, the distribution is switched vertically relative to the waveform direction for $\alpha = 2$ and 3, and the whole accuracy is less at least $\alpha = 4$, but it does not differ greatly. In *Scenario* 6, the distribution is switched as well as *Scenario* 5. The fidelity of the waveform is high at the center of the array for $\alpha = 4 - 8$. Furthermore, for $\alpha = 9$ and 10, the whole accuracy improved in the comparison area.

6 Conclusion

In this paper, we proposed that the Lamé function is useful for plane wave creation under cube-like loudspeaker arrays. Increasing the order of the Lamé function, the

faces are shaped in arrays. The accuracy is degraded in the case of plane wave direction and the face is parallel because the number of loudspeakers is a few for creating a plane wave while it is improved at a higher order of the Lamé function where at least two faces are accessible. We confirmed that it does not affect the creation of the plane waveform. By contrast, the creation area does not expand when the reproduction area inflates. This is caused by each loudspeaker assuming point source and floating in space. Considering an actual environment, we would predict that the direction of the sound radiation is limited because loudspeakers must be anchored in a speaker baffle. Consequently, the waveform will be interfered with by high order Lamé function.

References

[1] Omoto, A. and Kashiwazaki, H., "Hypotheses for constructing a precise, straightforward, robust and versatile sound field reproduction system," Acoustical Science and Technology, 41(1), pp. 151–159, 2020, doi:10.1250/ast.41.151.

[2] BS.775-4, I.-R., Multichannel stereophonic sound system with and without accompanying picture, 2022.

[3] BS.2051-3, I.-R., Advanced sound system for programme production, 2022.

[4] Pulkki, V., "virtual sound source positioning using vector base amplitude panning," journal of the audio engineering society, 45(6), pp. 456–466, 1997.

[5] Berkhout, A. J., de Vries, D., and Vogel, P., "Acoustic control by wave field synthesis," The Journal of the Acoustical Society of America, 93(5), pp. 2764–2778, 1993, ISSN 0001-4966, doi:10.1121/1.405852.

[6] a., G. M., "periphony: with-height sound reproduction," journal of the audio engineering society, 21, pp. 2–10, 1973.

[7] Williams, E. G. E. G., Fourier acoustics : sound radiation and nearfield acoustical holography / Earl G. Williams., Academic Press, San Diego, Calif, 1st edition edition, 1999, ISBN 1-281-03380-4.

[8] Ward, D. and Abhayapala, T., "Reproduction of a plane-wave sound field using an array of loudspeakers," IEEE Transactions on Speech and Audio Processing, 9(6), pp. 697–707, 2001, doi:10.1109/89.943347.

[9] Iwai, K., Suzuki, H., and Nishiura, T., "3-D Sound Image Reproduction Method Based on Spherical Harmonic Expansion for 22.2 Multichannel Audio," Applied Sciences, 12(4), 2022, ISSN 2076-3417, doi:10.3390/app12041994.

[10] Gielis, J., Lamé Curves and Surfaces, pp. 43–55, Atlantis Press, Paris, 2017, ISBN 978-94-6239-151-2, doi:10.2991/978-94-6239-151-2_4.

[11] Wierstorf et al., H., "Theory of Sound Field Synthesis," 2019, doi:10.5281/zenodo.2597215.

[12] Yamanaka, Y., Takeuchi, D., Kuze, D., Ikeda, Y., and Oikawa, Y., "Large-scale loudspeaker array system for sound field reproduction using high-speed 1 bit signal processing," Proceedings of Meetings on Acoustics, 29(1), p. 055005, 2017, ISSN 1939-800X, doi:10.1121/2.0000644.